Biophysical Journal, Volume 98

Supporting Material

Long-lived high strength states of ICAM-1 bonds to aL b2 integrin: I. lifetimes of bonds to recombinant aL b2 under force

Evan Evans, Koji Kinoshita, Scott I. Simon, and Andrew Leung

On-line Supporting Material

Long-lived high strength states of ICAM-1 bonds to $\alpha_L \beta_2$ integrin: I. lifetimes of bonds to recombinant $\alpha_L \beta_2$ under force

Evan Evans [†,‡,*] **, Koji Kinoshita** [†,‡] **, Scott Simon** [§] **, Andrew Leung** [‡]

[*] address correspondence to: evanse@bu.edu

[†] Biomedical Engineering, Boston University, Boston, MA 02215

[‡] Physics and Pathology, University of British Columbia, Vancouver, BC Canada V6T 2A6

[§] Biomedical Engineering, University of California, Davis CA 95616

Lifetimes of attachments measured over the course of a single force ramp experiment
Figure S1 A-C shows examples of attachment lifetimes plotted according to their sequence of measurement in three different ramp tests, which demonstrate the apparent lack of correlations amongst outliers (points above the dotted lines) used to characterize multiple attachments. Similar sets of data appear in Fig. 3A of the paper after truncation of the outliers and sorting in order of ascending lifetime.

Figure S1. Lifetimes for mICAM-1 bonds to recombinant $\alpha_L \beta_2$ on microspheres obtained in the course of three different force ramp experiments in 2mM solutions of Mn^{2+}. The data for a nominal force ramp $k_f V_{pull}$ = 10 pN/s appear in **A**, for 100 pN/s in **B** , and for 1000 pN/s in **C** (the measured ramp values appear in each legend along with the total number of attempts to form attachments). Outliers selected by Poisson statistics for truncation appear above the horizontal dotted lines and the limit of nonspecific controls are indicated by the lower solid lines. The pink stars note a change in chamber preparation.

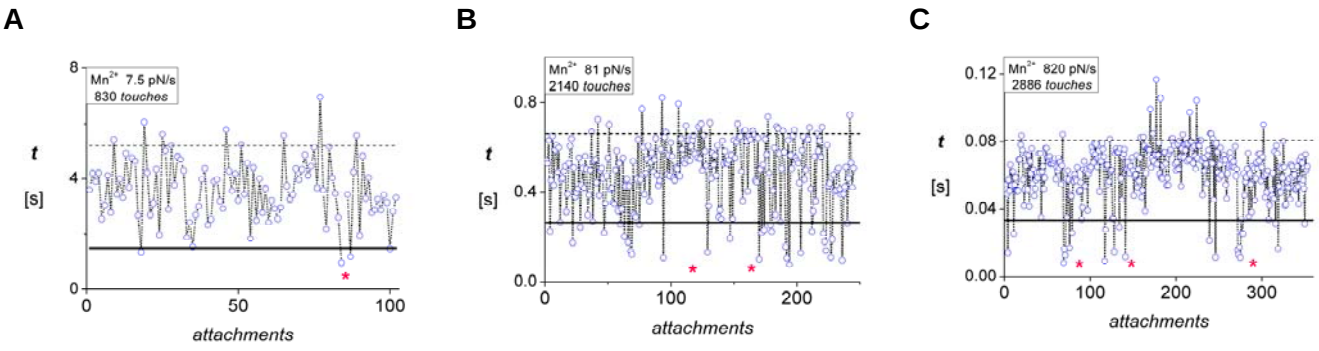

Other tests of ICAM-1 interactions with LFA-1

As mentioned in the introduction, both flow chamber techniques (*1*) and atomic force microscopy (*2*,*3*) have been used to study interactions of diICAM-1 with LFA-1 expressed on leukocytic cells in solutions of divalent metal cations. Of these two approaches, only tethering in flow chambers is designed to quantify lifetimes of bonds subjected to force. Because multiple bonds become very likely when cells or particles are arrested at high channel flow rates, the most reliable estimates for off rates in flow chamber tests are obtained under conditions of very slow flow. As a good example, Vitte et al. (*1*) studied lifetimes of Jurkats tethered to diICAM-1fc coated surfaces at a very low wall shear rate of ~3/s (estimated to produce ~1 pN pulling force). Over short time frames of 0-2 s, lifetimes were found to decay at rates of ~0.3-0.4/s while ten-fold slower rates characterized decay over longer time frames (~10 s), indicating at least two populations of tethered cells. Most likely, the initial rate of detachment characterized single-bonded tethers whereas the slower rate at longer times involved multiple-bonded tethers. At the same time given that the pulling forces might be a few pN, the stress-free off rate for these single-bonded tethers could be much slower than 0.3-0.4/s, depending on the actual level of detachment force.

In the case of AFM studies (*2*,*3*), off rates have been derived from analysis of forces measured during retraction of diICAM-1 coated substrates after contact with a leukocytic cell stuck to an AFM tip. Measured from AFM deflection during long traces of cell separation, many forces and apparent force rates for rupture events were collected at several retraction speeds, providing a spectrum of force histograms versus the force rates. As the method for analysis, the force peak (most frequent force f^*) in each histogram was correlated to the apparent force rate, which is expected to depend on how off rate changes with force (*4*), i.e. $[\partial(r_f/k_{off})/\partial f]_{f^*} = -1$. Hence, for constant ramps, f^* is proportional to $\ln(r_f)$ when the off rates match Bell's exponential model (*5*). The force scale and stress-free off rate k_o characterizing the exponential response are then the slope ($= 1/f_\beta$) and intercept ($= k_o f_\beta$) of a linear regime (*4*), i.e. $f^* = f_\beta \ln[r_f/(k_o f_\beta)]$. Probing diICAM-1 attachments to leukocytic cells in Mg^{2+}, initially 3A9 cells (*2*) and later Jurkats (*3*), two linear regimes were found in the AFM studies, beginning in both studies with identical weak increases in force (low slope) up to stress rates of ~2000 pN/s and subsequently crossing over to a very steep increase in force at stress rates > 10000 pN/s. Although qualitatively consistent our data plotted in Figs. 3D-E, the off rates derived from analysis of the AFM tests are factors of at least 10 to 100 fold lower at forces > 20 pN. Having introduced and used this type of approach for over a decade, we recognize its phenomenological usefulness in such studies but caution that it is unlikely to provide accurate measures of off rates, especially in the regime of small forces, when separation of large cell-surface contacts result in long periods of variable force loading to bonds and large force noise obscures quantitative accuracy.

Appendix I: Two-state transitions and the experimental assay for off rates

Critical to our method for data analysis, the statistics of bond lifetimes must represent a single population of pair-wise molecular interactions. Next, to model the interactions with two-state kinetics, the key requirement is that the dynamics of transitions between internal states along the pathway must be orders of magnitude faster than the overall time needed to reach the end state. Even so, consequences of fast internal transitions can still appear when exploring a large range of forces or applying fast force ramps as shown in the text.

Given two-state dynamics, the estimator for bound state probability, i.e. $S(t_i) \approx N(t_i)/N(0)$, characterizes the likelihood that single molecular complexes survive to a particular time t over the course of an experiment (i.e. multiple pulls), which defines the probability $S_1(t)$ of being in state 1. A first order Markov equation models the evolution of this initial state to a subsequent (unbonded) state $S_2(t)$, i.e.

$$dS_1(t)/dt = - k_{off}(t)\, S_1(t) + k_{on}(t)\, [1 - S_1(t)]$$
$$S_2(t) \equiv [1 - S_1(t)] \qquad \text{(AI-1)}$$

governed by the instantaneous frequencies for unbinding $k_{off}(t)$ and rebinding $k_{on}(t)$ transitions. With the initial condition $S_1(0) = 1$, the solution to Eq. AI-1 has the general form,

$$S_1(t) = \exp\{ -\textstyle\int_{0\to t} [k_{off}(t') + k_{on}(t')]\, dt' \}\ \int_{0\to t} k_{on}(t') \exp\{ \int_{0\to t'} [k_{off}(t'') + k_{on}(t'')]\, dt'' \}\, dt' \qquad \text{(AI-2)}$$

In probe experiments, application of pulling force with a "soft" spring κ_s significantly suppresses the rebinding rate as predicted by, i.e. $k_{on}(t) \approx k_{on}^{o} \exp[-f(t)^2/(2\kappa_s k_B T)]$. Hence, $k_{off}(t)$ quickly exceeds $k_{on}(t)$, reducing the two-state dynamics to a first-order decay process, $dS_1(t)/dt \approx - k_{off}(t)\, S_1(t)$, that depends only on cumulated frequency of dissociation, i.e. $S_1(t) \approx \exp[- \int_{0\to t} k_{off}(t')\, dt']$. As such, the probability density, $p_1(t) = - dS_1(t)/dt$, reflects the "instantaneous" rate, $k_{off}(t)\, S_1(t)$, at which the bound-state probability decreases; and the ratio of probability density/probability $p_1(t)/S_1(t)$ is the "instantaneous" off rate, $k_{off}(t)$. The histograms (ΔN_k) of events cumulated over discrete time differences Δt provide the key estimators for probability densities, $p_1(t_k) \approx (1/\Delta t)\, [\Delta N_k/N(0)]$, at the bin centers t_k. Interpolating amongst the array $N(t_i)$, we obtain the values $N(t_k)$ needed to establish the estimator for probability density/probability and the assay for off rates,

$$k_{off}(t_k) = p_1(t_k)/S(t_k) \approx (1/\Delta t)\, [\Delta N_k/N(t_k)] \qquad \text{(AI-3)}$$

Perhaps most significant, this generic assay for kinetic rates is valid even when transition rates vary over time, which allows the approach to be applied in all modes of force spectroscopy as long as the force rate is a deterministic function of time $r_f(t)$, i.e. increasing or decreasing or remaining constant. The force level corresponding to each off rate measurement is given by the integral of the force rate up to the time t_k, i.e. $f(t_k) = \int_{0\to tk} r_f(t)\, dt$. Moreover, since the estimator for probability density/probability is independent of the normalization $N(0)$, we can commence the analysis at any value of the initial time (or force), which allows us to simply ignore bins at low forces and short times in histograms contaminated by large numbers of nonspecific interactions. Extending the approach in our companion article II (Kinoshita et al., 2009), we show that three state dynamics need to be considered when dimeric ligands are involved.

As noted in the Results section, a related version of the assay described above for off rates follows from the analysis of force statistics, which has been described in Marshall et al. (*6*), Dudko et al. (*7*), and Evans et al. (*8*). Given a deterministic relation between force and time, it was shown some time ago that the instantaneous force rate, $r_f(t) = df(t)/dt$, transforms the

probability density of events in time to the probability density of events in force (*4*,*9*), i.e. $p_1(t)/r_f(t) \equiv p_1(f)$. Again dividing by probability, we obtain an assay for off rates in terms of the force statistics,

$$k_{off}(f_k) = r_f(f_k)\, p_1(f_k)/S(f_k) \approx [r_f(f_k)/\Delta f]\, [\Delta N_k/N(f_k)] \qquad \text{(AI-4)}$$

For a constant force ramp r_f, bin widths Δf in force histograms reduce to $r_f\, \Delta t$. However, when bonds are pulled through anharmonic elastic connections like polymers, the force rate is unsteady and changes with time (i.e. force). In this case, the density distribution for forces must be scaled at each time by the instantaneous force rate to obtain the distribution of events in time (*9*). The importance of unsteady loading and the generality of the assay for kinetic rates has been nicely demonstrated by Dudko et al. (*7*) using force distributions obtained for protein unfolding by AFM.

Appendix II: Transitions involving two activation barriers

Here we describe two simple models that produce a sequence of linear regimes in logarithmic plots of off rates versus force, each associated with one of two barriers. The first model is based on a single thermodynamic pathway that originates from state 1 (bound) then traverses an inner energy barrier via an intermediate (state 2) before finally passing the outer energy barrier to state 3 (unbound). An approximation for the off rate under conditions of changing force (see *10*) is provided by an expression involving two forward transition rates $k_{1\to2}$, $k_{2\to3}$ for passage of the barriers and the reverse rate $k_{1\leftarrow2}$ for return from the intermediate to the ground state,

$$k_{off} \approx k_{1\to2}\, k_{2\to3} /\{\, k_{1\to2} + k_{1\leftarrow2} + k_{2\to3} \,\} \qquad \text{(AII-1)}$$

Using Arrhenius phenomenology, we can convert Eq. AII-1 to a form that depends on rates of transition $k_{1\to2}$, $k_{1\to3}$ defined for dissociation from the ground state past each barrier and the ratio of forward/return rates at the inner barrier defined by the free energy of the intermediate state G_{IM} relative to the ground state, i.e.

$$k_{1\to2} = k_{o1} \exp[\Delta G_{B1}(f)/k_BT]$$

$$k_{1\to3} = k_{o2} \exp[\Delta G_{B2}(f)/k_BT] \qquad \text{(AII-2)}$$

$$k_{1\leftarrow2} / k_{1\to2} = \exp[G_{IM}/k_BT]$$

Approximating the forward rates of transition by exponential dependences on force, we express the changes in activation energies of the two barriers as, $\Delta G_{B1}(f)/k_BT = f/f_{\beta1}$, $\Delta G_{B2}(f)/k_BT = f/f_{\beta2}$, and define force-free prefactors for the rates as, k_{o1}, k_{o2}. Treated with a similar approximation, the reverse rate of transition is modeled by the relation, $k_{1\leftarrow2} / k_{1\to2} \approx \exp[G_{IM}^{o}/k_BT - f\,\Delta(1/f_{\beta})_{IM}]$. Thus, we use $k_{2\to3} = k_{1\to3}\,(k_{1\leftarrow2} / k_{1\to2})$ and the previous rate expressions to estimate the effective off rate dependence on force,

$$k_{off} \approx 1 /\{ \exp[-G_{IM}^{o}/k_BT + \Delta(1/f_{\beta})_{IM} - f/f_{\beta2}] / k_{o2} + \exp[-f/f_{\beta2}] / k_{o2} + \exp[-f/f_{\beta1}] / k_{o1} \} \qquad \text{(AII-3)}$$

In the context of the linear regimes indicated in Fig. 4C of the text, this single pathway expression for off rate will only closely match the behavior (cf. dotted curve in Fig. 4C) when the energy level of the intermediate state remains significantly above the ground state, i.e. $G_{IM}^{o}/k_BT - \Delta(1/f_{\beta})_{IM} \gg k_BT$ and $\exp[-G_{IM}/k_BT] \ll 1$. In this case, the off rate reduces to the harmonic mean of the two forward rates of barrier transition starting from the bound state, which is the reciprocal total time needed to pass both barriers,

$$k_{off} \approx 1 /\{ \exp[-f/f_{\beta2}] / k_{o2} + \exp[-f/f_{\beta1}] / k_{o1} \} \qquad \text{(AII-4)}$$

Neglecting retardation by metastable states, the approximation in Eq. AII-4 has been used to model more than one energy barrier in earlier force spectroscopy studies by our group (*4*,*11*) as well as in the studies of β_2 integrin interactions by AFM (*2*,*3*). [Note: a functionally-equivalent expression is found when the intermediate state remains below the ground state, i.e. $G_{IM}^{o}/k_BT - \Delta(1/f_{\beta})_{IM} \ll k_BT$. However, when subjected to force ramps, the approximation in Eq. AII-1 breaks down and it becomes necessary to solve the coupled non-linear equations describing the dynamics of each state (*10*).]

In contrast to the single pathway model, the rate of bond dissociation in the two-pathway model (*12*) involves transitions originating from two separate configuration states with occupancies S_1, S_2 that follow separate channels for dissociation as defined by rates k_1, k_2, i.e.

$$d(S_1+S_2)/dt = - k_1 S_1 - k_2 S_2 \qquad \text{(AII-5)}$$

Coupled by inner exchange, the evolution of the probability (S_1+S_2) for survival splits into two equations with exchange terms, $\pm (k_{21} S_2 - k_{12} S_1)$. In the absence of rebinding, these equations are given by,

$$\begin{aligned} dS_1/dt &= - k_1 S_1 - k_{12} S_1 + k_{21} S_2 \\ dS_2/dt &= - k_2 S_2 - k_{21} S_2 + k_{12} S_1 \end{aligned} \qquad \text{(AII-6)}$$

Treating the exchange as thermally equilibrated, a free energy difference ΔG_{21} between the two configurations defines the initial partition at $t = 0$,

$$\begin{aligned} k_{12} S_1 - k_{21} S_2 &\approx 0 \\ S_1/S_2 \approx k_{21}/k_{12} &\equiv \exp(\Delta G_{21}/k_B T) \end{aligned} \qquad \text{(AII-7)}$$

Thus, the fractional dissociation along pathways *1*,*2* and the occupancy of each state can be shifted mechanically when the applied force f couples to a length Δx_{12} that lowers the difference in energy ΔG_{21}. The effect leads to a switch in configurations, $k_{21}/k_{12} = \exp[(\Delta G_{21} - f \Delta x_{12})/k_B T]$, and in dissociation kinetics at a force $f_\otimes = \Delta G_{21}/\Delta x_{12}$. The width of the force response, $f_{12} = k_B T/\Delta x_{12}$, converts the thermodynamics of equilibration into a mechanical switching function,

$$R_S(f) = \exp[(f_\otimes - f)/f_{12}] \qquad \text{(AII-8)}$$

When thermally equilibrated in this way, a single force-dependent off rate $k_{off}(f)$ characterizes the combined rate of two-pathway dissociation,

$$\begin{aligned} k_{off}(f) &= \{ k_1(f) + \exp[-(f_\otimes - f/f_{12})]\, k_2(f) \} / \{ 1 + \exp[-(f_\otimes - f/f_{12})] \} \\ d[\ln(S_1+S_2)]/dt &\approx - k_{off}(f) \end{aligned} \qquad \text{(AII-9)}$$

The ratio $f_\otimes/f_{12}$ specifies the energy (in $k_B T$ units) needed to be over come by force to switch from configuration 1 to configuration 2. Again approximating the rates of transition $k_1(f)$,$k_2(f)$ by exponential dependences on force, we show correlations of Eq. AII-9 in Fig. 4C of the text (solid curves) to all of the off rate data obtained from tests in Mg^{2+} and Ca^{2+}. [The parameters used in the fits are listed below in Table 2.]

Table 2

"Approximate Parameters Characterizing New Branches of k_{off} at High Forces in Figure 4C"

metal cation [2 mM]	k_{o2}/k_o	$f_{\beta 2}$ [pN]	$f_{\otimes}$ [pN]
Mg^{2+}	~8 x 10^3	~68	70
Mn^{2+}	~9 x 10^3	~68	70
Ca^{2+}	~72	~68	50

REFERENCES

1. Vitte, J., A. Pierres, A-M. Benoliel, and P. Bongrand. 2004. Direct quantification of the modulation of interaction between cell- or surface-bound LFA-1 and ICAM-1. *J. Leukoc. Biol.* 76: 594-602.

2. Zhang, X., Wojcikiewicz, E.P., and V.T. Moy. 2002. Force spectroscopy of the Leukocyte Function-Associated Antigen-1/Intercellular Adhesion Molecule-1 interaction. *Biophys. J.* 83: 2270-2279.

3. Wojcikiewicz, E.P., Abdulreda, M.H., Zhang, X., and V.T. Moy. 2006. Force spectroscopy of LFA-1 and its ligands ICAM-1 and ICAM-2. *Biomacromolecules* 7: 3188-3195.

4. Evans, E., and K. Ritchie. 1997. Dynamic strength of molecular adhesion bonds. *Biophys. J.* 72: 1541–1555.

5. Bell, G.I. 1978. Models for the specific adhesion of cells to cells. *Science* 200: 618-627.

6. Marshall, B.T., K.K. Sarangapani, J. Lou, R.P. McEver, and C. Zhu. 2005. Force history dependence of receptor-ligand dissociation. *Biophys. J.* 88: 1458-1466.

7. Dudko, O.K., Hummer, G. and A. Szabo. 2008. Theory, analysis, and interpretation of single-molecule force spectroscopy experiments. *Proc. Natl. Acad. Sci.* 105: 15755-15760.

8. Evans, E., Halvorsen, K., Kinoshita, K. and W.P. Wong. 2009. A new approach to analysis of single molecule force experiments. In Handbook of Single-Molecule Biophysics. P. Hinterdorfer and A.M. van Oijen (eds). Chapter 20 (Springer Science, NY).

9. Evans, E. and Ritchie, K. Strength of a Weak Bond Connecting Flexible Polymer Chains. *Biophys. J.* 76:2439-2447, 1999.

10. Evans, E. and P. Williams. 2002. Dynamic force spectroscopy: I. single bonds. In Physics of Bio-Molecules and Cells, *Les Houches: Ecoles d'Ete de Physique Theorique*, (EDP Sciences – Springer) Vol. 75, pp. 145 - 185.

11. Merkel, R., Nassoy, P., Leung, A., Ritchie, K. and Evans. E. Energy Landscapes of Receptor-Ligand Bonds Explored with Dynamic Force Spectroscopy. *Nature* 397:50-53, 1999.

12. Evans, E., A. Leung, V. Heinrich, and C. Zhu. 2004. Mechanical switching and coupling between two dissociation pathways in a P-selectin adhesion bond. *Proc. Natl. Acad. Sci. USA* 101: 11281-11286.